Frequency estimator to improve H-scan tissue characterization

Jihye Baek
Department of Radiology
Stanford University School of Medicine
Stanford, CA, USA
baekjh@stanford.edu

Thurston Brevett
Department of Radiology
Stanford University School of Medicine
Stanford, CA, USA
tbrevett@stanford.edu

Dongwoon Hyun
Department of Radiology
Stanford University School of Medicine
Stanford, CA, USA
dhyun@stanford.edu

Ahmed El Kaffas
Department of Radiology
University of California
San Diego, La Jolla, CA, USA
aelkaffas@ucsd.edu

Kevin J. Parker
Department of Electrical and Computer Engineering
University of Rochester
Rochester, NY, USA
kevin.parker@rochester.edu

Jeremy Dahl
Department of Radiology
Stanford University School of Medicine
Stanford, CA, USA
jjdahl@stanford.edu

2024 IEEE Ultrasonics, Ferroelectrics, and Frequency Control Joint Symposium (UFFC-JS) | 979-8-3503-7190-1/24/$31.00 ©2024 IEEE | DOI: 10.1109/UFFC-JS60046.2024.10793751

***Abstract*— H-scan is a promising quantitative ultrasound method that uses a red/blue color display to illustrate the frequency of backscattered signal, representative of tissue properties. It is based on matched filters of different frequencies, but has a noisy pattern due to the broad spectral distribution of ultrasound. We suggest an improved adaptive frequency estimator reducing the noise in homogeneous regions but maintaining sharpness at boundaries.**

The proposed frequency estimator utilizes 2D autocorrelation with a matched filter. This estimator provides an a priori estimate of the spatial distribution of frequencies using a matched-filter-based frequency estimation. The heterogeneity of the estimated frequencies is then used to define a 2D weighting function for a second frequency estimation stage. Autocorrelation, borrowing the concept of Loupas's blood velocity measure, is then used to measure the axial frequency components with a 2D spatial kernel. We use a weighted summation in the autocorrelation based on the spatial frequency distribution within the 2D kernel. The proposed frequency estimator was compared with currently available frequency estimators, including short time Fourier transform, H-scan matched filter, and autocorrelation. We examined the performance of the frequency estimators using Field II simulations and in human subjects with hepatic steatosis.

Field II simulation results showed that our adaptive estimator can reduce the noisy texture pattern in H-scan for homogeneous regions while maintaining delineation of boundary interfaces, whereas other estimators are only capable of reduce the noise or maintaining boundary delineation. We applied our adaptive estimator to *in vivo* human liver, demonstrating improved visualization of H-scan images while reducing the noisy texture pattern and improving differentiation of steatotic liver from gallbladder/skin layer.

Keywords—H-scan, Frequency estimator, Tissue characterization, Quantitative ultrasound

I. Introduction

H-scan has shown promise in tissue characterization, enabling identification of a variety of diseases in animal models and human subjects by showing differentiation between diseases and disease progression [2-8].

The original H-scan method evaluates the output of a pair of matched filters, one each at a high and low frequency [9]. Recently, a fine-tuned H-scan approach has been proposed using 256 matched filters to obtain a greater spectral composition, enabling improved illustration of tissue signatures [1]. Because ultrasound echoes are composed of a broad range of frequencies, displaying H-scan as a map of the local frequency results in a noisy texture pattern. Thus, H-scan is shown on a binarized red/blue color map so as to identify gross shifts in tissue properties rather than an exact frequency shift. In this study, we focus on enhancing the accuracy of frequency estimation to improve H-scan tissue characterization.

Other methodologies for localized frequency estimation include the Short-time Fourier transform (STFT), matched filter analysis (e.g., H-scan [1]), and axial autocorrelation (adapted from Loupas's 2D autocorrelator for blood flow [10]). For the STFT and 2D autocorrelator, setting an appropriate window size for the estimation kernel is critical, whereas the matched filter does not require a window. This noisy texture pattern from these estimators can be suppressed by low-pass filtering or setting a larger window for the STFT/autocorrelator, although there is a trade-off between estimator variance and resolution.

Here we propose an adaptive frequency estimator that takes advantage of the resolution of the matched filter approach with the lower variance of the 2D autocorrelation approach. We evaluated the performance of the estimator using Field II simulation and an *in vivo* study. The performance of proposed method was compared with the STFT, H-scan matched filter, and 2D autocorrelator.

II. Methods

A. Adaptive Frequency Estimator

The proposed adaptive frequency estimator is a modified 2D autocorrelator that utilizes a matched filter to search homogeneity/heterogeneity of the frequency distribution. The adaptive frequency estimator calculates the frequency ($\hat{f}$) from the axial/temporal autocorrelation of a discrete signal, $R(\tau) = A(\tau)e^{\hat{j}\phi(\tau)}$ with discrete time index τ. The frequency ($\hat{f}$) can be estimated using the correlation at lag 1 ($\tau = 1$) by:

$$\hat{f} = \frac{1}{2\pi}\phi(1). \quad (1)$$

Let $h(n) \equiv IQ(n) \cdot IQ^*(n-1)$ for a sample index n, and IQ represents the in phase and quadrature data combined as complex numbers. Here, we use the autocorrelation at lag 1 ($\tau = 1$) in a weighted summation:

$$R(1) = \sum_{n \in ROI} W(n) \cdot [IQ(n) \cdot IQ^*(n-1)] = \sum_{n \in ROI} W(n) \cdot h(n) \quad (2)$$

where $W(n)$ is the weight for each $h(n)$ in a region of interest (ROI). For the traditional autocorrelation, $W(n) = 1$ for all n. Here, we adaptively sum $h(n)$ based on the frequency distribution within a box ROI with $W(n)$ = 2D circularly Gaussian distribution with $\sigma(n)$ where $\sigma(n)$ is the standard deviation of the Gaussian distribution.

The matched filter in H-scan [1] is first used to estimate the frequency distribution ($\hat{f}_{Matched}$). Next, the homogeneity within an ROI$_n$ centered at sample index n is defined as the averaged difference between $\hat{f}_{Matched}(n)$ and $\hat{f}_{Matched}(i)$, where $i \in \text{ROI}_n$. The homogeneity is linearly mapped to σ, the standard deviation of the Gaussian distribution, defining $W(n)$; For lower homogeneity, we assigned low $\sigma(n)$ for $W(n)$; whereas we assigned higher $\sigma(n)$ for a homogeneous area. The frequency from the adaptive estimator is borrowed from the concept of Loupas's blood flow velocity estimator [10], which estimates the ensemble directional frequency in the axial direction:

$$\hat{f} = \frac{1}{2\pi}\tan^{-1}\left(\frac{\sum_{n\in ROI}[Im(W(n)\cdot h(n))]}{\sum_{n\in ROI}[Re(W(n)\cdot h(n))]}\right). \quad (3)$$

TABLE I. FIELD II SIMULATION PROPERTIES

Property	Value
Transmit Frequency	3.15 MHz
Attenuation Coefficient	0 dB/MHz/cm
Cycles	2
Sampling Frequency	100 MHz
# Elements	129 Elements
Kerf	24 μm
Pitch	513 μm

B. Field II Simulation

We performed Field II simulations [11] to evaluate our adaptive frequency estimator. The Field II simulation parameters are summarized in Table 1. RF data with 0 dB/MHz/cm attenuation were simulated and then processed to generate artificial frequency shift by:

$$IQ(t) = RF\ (t) \cdot \exp\left(-j2\pi f_{shift}t\right). \quad (4)$$

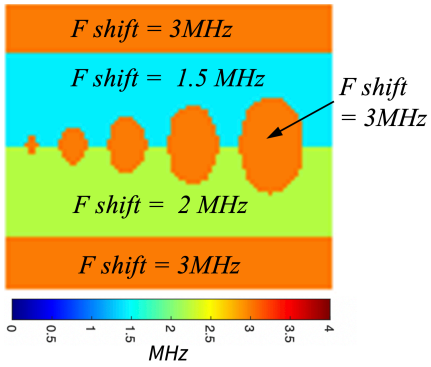

Fig. 1. Validation phantom simulated by Field II and artificial frequency shift.

where f_{shift} is an artificial frequency shift. The simulated phantom is visualized in Fig. 1.

C. In vivo Study

RF data from a patient with a stage 3 steatotic liver from a previous Stanford IRB approved protocol with informed consent were obtained. The stage 3 steatosis case is metabolic dysfunction-associated fatty liver disease (MAFLD). The patient liver pathology was confirmed by magnetic resonance imaging-derived proton density fact fraction (MRI-PDFF) measures.

D. Frequency Estimator Validation

The performance of our proposed adaptive frequency estimator was compared with currently available frequency estimators, including short time Fourier transform (STFT), the matched filter based estimator from H-scan [1], and 2D autocorrelation without adaptive weighting.

III. RESULTS

A. Field II Simulation

Field II simulation results are displayed in Fig. 2: from left to right, the ground truth, STFT, matched filter, median filtered STFT, median filtered matched filter, 2D autocorrelation, and the proposed estimator. The same 2D kernel size was applied to the median filter, autocorrelation, and the proposed method. ROI 1 includes the entire image,

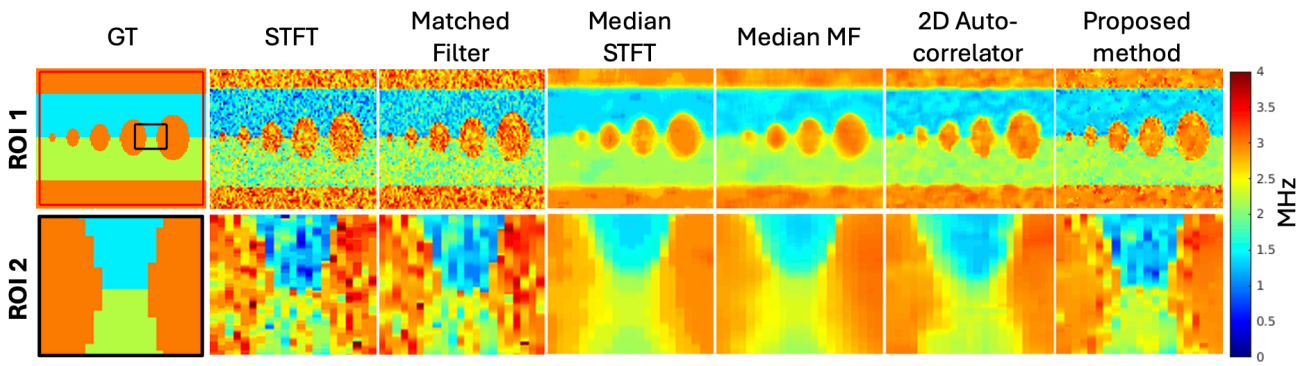

Fig. 2. Simulated phantom results. *GT: ground truth, STFT: short time Fourier transform, Median STFT: median filtered STFT, Median MF: median filtered matched filter.

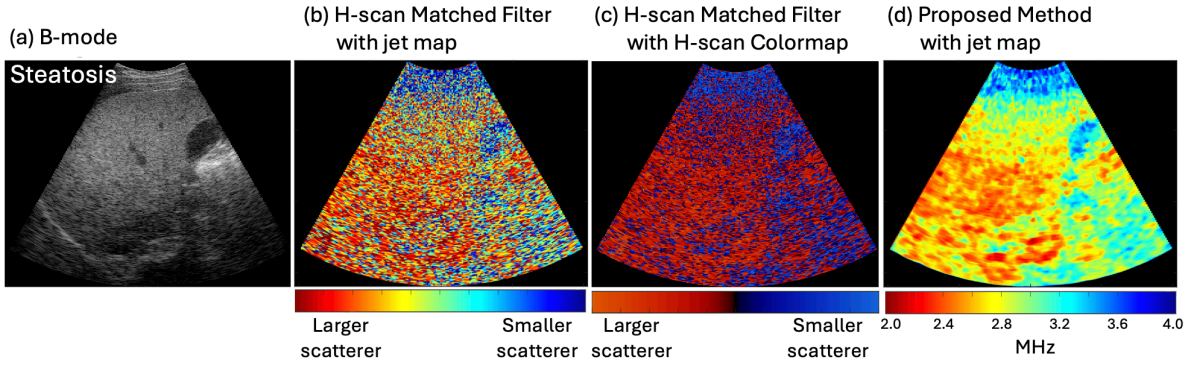

Fig. 3. *In vivo* frequency estimation results applied to H-scan matched filter analysis[1] and our proposed method for a steatotic liver. (a) B-mode (b) H-scan matched filter analysis [1] with jet color map (c) H-scan matched filter analysis [1] with H-scan binarized colormap (d) the proposed frequency estimator with jet colormap.

and ROI 2 only includes the area denoted by the black box. The STFT and matched filter showed sharper boundary area transitions but a salt-and-pepper noise texture. The median-filtered STFT, median-filtered matched filter, and the 2D autocorrelator results showed reduced noise at the expense of boundary sharpness. The proposed approach shows low estimator variance in the homogeneous area and sharper boundary delineation.

B. In vivo Study

Fig 3 shows an example of a stage 3 steatotic human liver: (a) B-mode, (b) matched filter H-scan [1] with jet colormap, (c) H-scan matched filter [1] with H-scan binarized colormap, and (d) H-scan with the proposed frequency estimator jet colormap. Applying the jet colormap to the H-scan matched filter frequency estimator results (Fig. 3 (b)) in noisy frequency measures. While the binarized colormap enabled H-scan to better visualize progression of diseases, such as hepatic steatosis [8] and pancreatic cancer metastasis in liver [12], quantification of disease progression is assessed by the ratio of red to blue. The non-binarized maps allow comparison of the magnitude of the frequency shift, but the noisy texture pattern makes this estimation difficult. As shown in Fig. 3 (d), our proposed frequency estimator reduces the noise pattern while avoiding loss in resolution of the H-scan image, without requiring a binarized colormap for H-scan. Thus, it shows better visual differentiation between tissues, such as differentiation of steatotic liver from gallbladder/skin layer while simultaneously providing a quantitative value for tissue characterization.

As shown in Fig. 3 (c), H-scan typically is illustrated as relatively larger and smaller scatterers, which is an ambiguous measure without a quantitative value. Our results in Fig. 3 (d) show a clear quantitative value of frequency measures.

ACKNOWLEDGMENT

This work was supported by National Institutes of Health grant R01-EB027100 and Stanford School of Medicine Dean's Fellowship.

REFERENCES

[1] K. J. Parker, and J. Baek, “Fine-tuning the H-scan for discriminating changes in tissue scatterers,” Biomedical physics & engineering express, vol. 6, no. 4, pp. 045012, 2020.

[2] J. Baek, S. S. Poul, T. A. Swanson et al., “Scattering signatures of normal versus abnormal livers with support vector machine classification,” Ultrasound in Medicine & Biology, vol. 46, no. 12, pp. 3379-3392, 2020.

[3] J. Baek, S. S. Poul, L. Basavarajappa et al., “Clusters of ultrasound scattering parameters for the classification of steatotic and normal livers,” Ultrasound in Medicine & Biology, vol. 47, no. 10, pp. 3014-3027, 2021.

[4] J. Baek, L. Basavarajappa, K. Hoyt et al., “Disease-specific imaging utilizing support vector machine classification of H-scan parameters: assessment of steatosis in a rat model,” IEEE Transactions on Ultrasonics, Ferroelectrics, and Frequency Control, vol. 69, no. 2, pp. 720-731, 2021.

[5] J. Baek, S. S. Qin, P. A. Prieto et al., "H-scan imaging and quantitative measurement to distinguish melanoma metastasis." 2021 IEEE International Ultrasonics Symposium (IUS), pp. 1-4.

[6] J. Baek, A. M. O’Connell, and K. J. Parker, “Improving breast cancer diagnosis by incorporating raw ultrasound parameters into machine learning,” Machine Learning: Science and Technology, vol. 3, no. 4, pp. 045013, 2022.

[7] J. Baek, E. Hysi, X. He et al., "Detecting kidney fibrosis using H-scan." 2022 IEEE International Ultrasonics Symposium (IUS), pp. 1-3.

[8] J. Baek, A. El Kaffas, A. Kamaya et al., “Multiparametric quantification and visualization of liver fat using ultrasound,” WFUMB Ultrasound Open, vol. 2, no. 1, pp. 100045, 2024.

[9] K. Parker, “Scattering and reflection identification in H-scan images,” Physics in Medicine & Biology, vol. 61, no. 12, pp. L20, 2016.

[10] T. Loupas, J. Powers, and R. W. Gill, “An axial velocity estimator for ultrasound blood flow imaging, based on a full evaluation of the Doppler equation by means of a two-dimensional autocorrelation approach,” IEEE transactions on ultrasonics, ferroelectrics, and frequency control, vol. 42, no. 4, pp. 672-688, 1995.

[11] J. A. Jensen, "Field: A program for simulating ultrasound systems."

[12] J. Baek, R. Ahmed, J. Ye et al., “H-scan, Shear Wave and Bioluminescent Assessment of the Progression of Pancreatic Cancer Metastases in the Liver,” Ultrasound in Medicine & Biology, vol. 46, no. 12, pp. 3369-3378, 2020.